Title: iPSC-based drug repositioning identifies the Src/c-Abl pathway as a therapeutic target for ALS motor neurons

Authors: Keiko Imamura[1]*, Yuishin Izumi[2], Akira Watanabe[1], Kayoko Tsukita[1], Knut Woltjen[1,3], Takuya Yamamoto[1,4], Akitsu Hotta[1,4,5], Takayuki Kondo[1], Shiho Kitaoka[1], Akira Ohta[1], Akito Tanaka[1], Dai Watanabe[6], Mitsuya Morita[7], Hiroshi Takuma[8], Akira Tamaoka[8], Tilo Kunath[9], Selina Wray[10], Hirokazu Furuya[11], Takumi Era[12], Kouki Makioka[13], Koichi Okamoto[14], Takao Fujisawa[15], Hideki Nishitoh[16], Kengo Homma[15], Hidenori Ichijo[15], Jean-Pierre Julien[17], Nanako Obata[18], Masato Hosokawa[18], Haruhiko Akiyama[18], Satoshi Kaneko[19], Takashi Ayaki[20], Hidefumi Ito[21], Ryuji Kaji[4], Ryosuke Takahashi[20], Shinya Yamanaka[1,22], Haruhisa Inoue[1†]

Affiliations:

1 Center for iPS Cell Research and Application (CiRA), Kyoto University, Kyoto 606-8507, Japan

2 Department of Clinical Neuroscience, The University of Tokushima Graduate School, Tokushima, 770-8503, Japan

3 Hakubi Center for Advanced Research, Kyoto University, Kyoto 606-8501, Japan

4 Institute for Integrated Cell-Material Sciences (WPI-iCeMS), Kyoto University, Kyoto 606-8507, Japan

5 PRESTO, JST, Saitama 332-0012, Japan

6 Department of Biological Sciences, Graduate School of Medicine, Kyoto University, Kyoto 606-8501, Japan

confidential

7 Division of Neurology, Department of Internal Medicine, Jichi Medical University, Shimotsuke, 329-0498, Japan

8 Department of Neurology, Institute of Clinical Medicine, University of Tsukuba, Tsukuba 305-8576, Japan

9 MRC Centre for Regenerative Medicine, School of Biological Sciences, University of Edinburgh, 5 Little France Drive, Edinburgh, EH16 4UU

10 Department of Molecular Neuroscience, UCL Institute of Neurology, Queen Square, London WC1N 3BG

11 Department of Neurology, Kochi Medical School, Kochi University, 783-8505, Japan

12 Department of Cell Modulation, Institute of Molecular Embryology and Genetics, Kumamoto University, Kumamoto, 860-0811, Japan

13 Department of Neurology, Gunma University Graduate School of Medicine, Maebashi 371-8511, Japan

14 Geriatrics Research Institute and Hospital, Maebashi, 371-0847, Japan

15 Cell Signaling, Graduate School of Pharmaceutical Sciences, The University of Tokyo, Bunkyo-ku, Tokyo 113-0033, Japan

16 Department of Medical Sciences, University of Miyazaki, 889-1601, Japan

17 Department of Psychiatry and Neurosciences, Research Centre of IUSMQ, Laval University, Quebec, Canada

18 Tokyo Metropolitan Institute of Medical Science 2-1-6 Kamikitazawa, Setagaya-ku, Tokyo 156-8506, Japan

19 Department of Neurology, Kansai Medical University, Hirakata, 573-1191, Japan

confidential

20 Department of Neurology, Graduate School of Medicine, Kyoto University, Kyoto 606-8507, Japan

21 Department of Neurology, Wakayama Medical University, Kimiidera, Wakayama 641-8509, Japan

22 Gladstone Institute of Cardiovascular Disease, San Francisco, CA 94158, USA

† To whom correspondence should be addressed.

One sentence summary:

Patient iPSC-based models indicate Src/c-Abl inhibitors as anti-ALS therapeutics.

confidential

Abstract

Amyotrophic lateral sclerosis (ALS), a fatal motor neuron (MN) disease causing progressive MN death, still has no effective therapeutics. Here we developed a phenotypic screen to reposition existing drugs with a readout of MN survival using ALS patient induced pluripotent stem cells (iPSCs) with mutations in Cu/Zn superoxide dismutase 1 (mutant SOD1). Results of the screen showed that over half of the hit drugs were included in the Src/c-Abl-associated signaling pathway. Src/c-Abl inhibitors increased the survival rate of ALS MNs, and a knock-down approach rescued ALS MNs. One of these drugs improved impaired autophagy, reduced misfolded SOD1 protein, and attenuated the energy shortage with altered mitochondria-relevant gene expression as detected by single-cell transcriptome analysis of ALS MNs. This drug was also effective for other genetic types of iPSC-derived MNs including mutant TAR DNA-binding protein 43 kDa (TDP-43), C9orf72 repeat expansion-associated familial ALS, and sporadic ALS. Furthermore, the Src/c-Abl inhibitor extended the survival period of mutant SOD1-associated ALS model mice. Therefore, our chemical-biology approach with iPSC-based drug repositioning could identify both candidate drugs and a converged molecular pathway for ALS therapeutics.

confidential

Introduction

Amyotrophic lateral sclerosis (ALS) is a neurodegenerative disease that causes progressive loss of motor neurons (MNs) [1, 2]. The disease progression is fast and there is no radical treatment. Most cases are classified as sporadic ALS (SALS), while about 10% are familial (FALS). Approximately 25% of the FALS cases are associated with mutations in *Cu/Zn superoxide dismutase 1* (*mutant SOD1*) [3]. Although mutant SOD1 transgenic mice recapitulate ALS phenotypes [4] and have been used for preclinical study of ALS drug development, only a limited number of compounds have been tested. Thus, we developed a phenotypic screening assay for testing a number of compounds with a readout of ALS MN survival. In previous studies of ALS, many kinds of causative genes were discovered and multiple molecular pathological hypotheses were proposed. However, it is clear that MN death is an undisputed common phenotype in the heterogeneous disease ALS [1, 2]. After the discovery of iPSC technology, many screening platforms targeting ALS have been developed [5-11]. In this study, we introduced transcription factors using the *piggyBac* vector system [12] to generate disease MNs with scale merit and simplicity for MN generation. In the phenotypic assay, since it was deemed useful to accelerate therapeutic development, we repositioned existing drugs [13] and found that several Src/c-Abl inhibitors attenuated ALS MN degeneration.

Src and c-Abl are ubiquitous non-receptor tyrosine kinases (RTKs) that were identified as the mammalian homologs of the oncogene products of Rous sarcoma virus and Abelson murine leukemia virus, respectively. Activation of Src, which is associated with cell proliferation, angiogenesis, apoptosis and invasion, has been observed in cancers, and it is

confidential

considered a target of cancer therapy [14]. Bcr-Abl fusion protein, one of the oncogenic forms of c-Abl fusion kinase, is known to cause chronic myelogenous leukemia (CML) and Philadelphia chromosome-positive adult acute lymphoblastic leukemia (Ph+ALL), and c-Abl inhibitors were developed as anti-CML drugs [15]. Src/c-Abl is associated with various cellular functions [16, 17], and several studies have shown the involvement of Src family proteins and c-Abl in neurodegenerative diseases [18-24].

In the present study, we repositioned existing drugs using mutant SOD1-mediated ALS iPSCs and identified multiple anti-Src/c-Abl cancer drugs, investigated the mechanism of Src/Abl inhibitors in ALS MNs, and demonstrated that Src/Abl inhibition attenuated MN death with a reduction of misfolded protein accumulations. These drugs were also effective for other genetic forms of ALS patient MNs and for ALS model mice, indicating that the Src/c-Abl pathway could be viewed as a converged therapeutic target of ALS MNs.

Results

To screen many compounds with MN vulnerability as a readout phenotype using patient iPSCs, we required large-scale maturation-aligned MNs. We developed MN differentiation methods by transducing 3 transcription factors, *LIM homeobox protein 3 (Lhx3)*, *neurogenin 2 (Ngn2)*, and *ISL LIM homeobox 1 (Isl1)*. These factors were reported to induce mature spinal MNs from neural precursor cells using adenovirus vectors [25]. A polycistronic vector containing *Lhx3*, *Ngn2*, and *Isl1* under control of the tetracycline operator was introduced into iPSCs (fig. S1A-D and table S1 and S2) using the *piggyBac* vector, and vector-introduced clones were established as stable iPSC clones after neomycin selection. After

confidential

doxycycline treatment, MNs were generated from iPSCs within 7 days (Fig. 1A). The generated MNs showed MN markers (Fig. 1B and C) and functional property (Fig. 1D-F and fig. S2A-C).

To establish an ALS MN phenotypic screening system, we generated iPSCs from ALS patients with a mutation of L144FVX in SOD1 gene (ALS1) (fig. S1A-D) and corrected the mutation in the established iPSCs using CRISPR-Cas9 to generate isogenic control (corrected ALS1) (fig. S2D-F). We differentiated iPSCs into MNs using transcription factors, and a MN marker, HB9-positive cells were 62.3±2.3% in control, 63.4±1.3% in corrected ALS1-1, and 60.3±2.8% in ALS1 (Fig. 1G and fig. S2G). In the generated MNs, we observed accumulations of misfolded SOD1 protein (Fig. 1H and I and fig. S2H and I), which plays a pathological role in mutant SOD1-associated ALS [26, 27]. Furthermore, we found vulnerability in ALS MNs compared with control MNs including mutation-corrected isogenic control (Fig. 1J and K).

Using this cellular model, we set up compound screening with a readout of the survival of ALS MNs. iPSCs were differentiated to MNs for 7 days, and chemical compounds were added for another 7 days, following evaluation of the surviving MNs by high-content analysis using immunostaining of βⅢ-tubulin, since nearly 100% of βⅢ-tubulin-positive neurons expressed HB9 (Fig. 2A and fig. S2J and K). Assay performance was determined by calculating the Z' factor (Z' factor = 0.42 ± 0.30 (mean ± SD)). For positive control assays, cells were treated with 50 μM kenpaullone, which was identified as a candidate drug for ALS [28], and we confirmed its positive effect; in negative control assays, the cells were treated with vehicle (DMSO). We conducted through-put screening of 1,416 compounds that

confidential

included existing drugs both on the market and undergoing clinical trials. The results of the screening are shown in Fig. 2B. Hit compounds were defined as over 3 standard deviations (3SD) from negative controls, and 27 compounds were identified as hits (hit ratio 1.7%) (table S3). Representative figures showing the neuroprotective effect of hit drugs are shown in Fig. 2C. We were able to confirm dose-dependency of the protective effect of some hit drugs (Fig. 2D).

Fourteen of the 27 hits were included in the Src/c-Abl-associated pathway (Fig. 2E). Thus, we focused on Src/c-Abl as a common target of these hit drugs in ALS MNs. We re-evaluated other Src/c-Abl inhibitors in non-hit drugs, and confirmed that they also presented a protective effect, although with lesser efficacy compared with hit drugs (fig. S3A). Furthermore, knock-down of Src or c-Abl promoted the survival of MNs (Fig. 2F), and the knock-down effects were cancelled by siRNA-resistant forms of Src or c-Abl overexpression (fig. S3B and C). These results demonstrated Src and c-Abl as therapeutic targets of ALS MNs. Among Src/c-Abl inhibitors of the hit drugs, we focused on drugs that have direct inhibitory activity for Src/c-Abl, such as bosutinib and dasatinib. Bosutinib presented dose-dependency on MN protection without the bell-shaped responses observed with dasatinib, and the protective effect was exhibited at lower dose compared with other hit drugs in vitro. From these results, we selected bosutinib for further investigation.

We investigated the protein level and phosphorylation of Src/c-Abl in ALS MNs. Phosphorylation of Src/c-Abl was increased in mutant SOD1 MN culture compared with control, and treatment with bosutinib decreased phosphorylation as detected by western blot analysis (Fig. 2G and H). Typical immunocytochemistry figures of phosphorylated Src (p-

confidential

Src)/phosphorylated c-Abl (p-c-Abl) are presented in Fig 2I. Using ELISA, we also confirmed that phosphorylation of Src/c-Abl was increased in mutant SOD1 MN culture compared with control, and treatment with bosutinib decreased them (Fig. 2J). Next, we evaluated the protein level and phosphorylation of Src/c-Abl in other types of cells. ALS astrocytes generated from iPSCs (fig. S3D) and ALS iPSCs exhibited increased phosphorylation of Src without increased phosphorylation of c-Abl (fig. S3E-H).

To analyze the protective mechanism of bosutinib on ALS MNs, we investigated misfolded protein degradation. We found that p62 levels were elevated in ALS MNs, which were then reduced by bosutinib treatment, and the change of the LC3-II/LC3-I ratio, suggestive but not definitively pointing to an autophagic effect, in ALS MNs was also attenuated by bosutinib treatment (Fig. 3A-C). To confirm whether the autophagy process was associated with ALS MNs, we investigated the effect of the inhibition of mTOR. The mTOR inhibitor rapamycin, which is known to promote autophagy, and mTOR siRNA increased MN survival (Fig. 3D and E), suggesting that autophagy was impaired in ALS MNs. Then, to investigate whether the protective effect of bosutinib is associated with the autophagy pathway, we added autophagy inhibitors, LY294002 and chloroquine, to MNs with bosutinib treatment. These autophagy inhibitors partially blocked the protective effect of bosutinib (Fig. 3F). Thus, our data suggested that the protective effect of bosutinib was associated with the promotion of autophagy. Furthermore, we found that bosutinib treatment reduced the misfolded SOD1 protein levels in ALS MNs by western blotting (Fig. 3G) and ELISA (Fig. 3H) without decreasing SOD1 mRNA expression levels (Fig. 3I). ALS MN culture also presented a decreasing ATP level, and bosutinib had an attenuating effect on the

confidential

shortage of intracellular ATP (Fig. 3J). These data suggested that bosutinib promoted the degradation of misfolded SOD1 protein and improved cellular energy shortage. To further explore the molecular background of ALS MNs, transcriptome analysis was performed using single-cell RNA sequencing (table S4 and S5). We conducted Gene Set Enrichment Analysis (GSEA) to reveal the biological significance of differentially expressed genes between control and ALS MNs. We found that the increase in mRNA expressions was associated with TCA cycle and respiratory electron transport in ALS MNs, indicating compensation for energy shortage (Fig. 3K). After treatment with bosutinib, the mRNA expressions associated with TCA cycle and respiratory electron transport were decreased in ALS MNs (fig. S4).

Furthermore, we evaluated the effects of Src/c-Abl inhibitor on other genetic types of familial ALS MNs including mutant TDP-43-, C9orf72 repeat expansion-associated familial ALS, and on sporadic ALS. Diagnosis of familial ALS was confirmed by genotype (Fig. S1A), and sporadic ALS was examined by re-sequencing using patient fibroblasts (table S2). TDP-43 inclusions were observed in spinal MNs of a SALS patient (SALS1) by postmortem pathological analysis. MNs were generated from each iPSC (Fig. 4A), and treatment with bosutinib increased surviving MNs in the different types of familial ALS and a part of sporadic ALS (Fig. 4B). Treatment with bosutinib decreased accumulations of abnormal proteins in MNs of familial and sporadic ALS (fig. S5A-C).

To analyze whether Src/c-Abl inhibitor is effective in vivo, we administered bosutinib to mutant SOD1 transgenic (Tg) mice, a known model for mutant SOD1-asssociated ALS. To investigate the effect of Src/c-Abl inhibitor on MN degeneration in vivo, the same as our in vitro ALS model, treatment with bosutinib (5mg/kg/day) by intraperitoneal injection was

confidential

started at age of 8 weeks, and was continued until 13 weeks. Bosutinib delayed disease onset (Fig. 4C) and extended the survival period of mutant SOD1 Tg mice (Fig. 4D). Src/c-Abl were inhibited (fig. S5D), and misfolded SOD1 proteins in spinal cord were decreased in bosutinib-treated mutant SOD1 Tg mice compared with vehicle treatment (Fig. 4E). The number of MNs was significantly higher in bosutinib-treated mutant SOD1 Tg mice compared with vehicle treatment (Fig. 4F and G). These results indicated that Src/c-Abl inhibition protected MNs from misfolded SOD1-mediated neurodegeneration in vivo. These data were compatible with previous reports of nilotinib/bosutinib treatment attenuating misfolded TDP-43 protein levels in other ALS model mice [29], and that treatment with another Src/c-Abl inhibitor, dasatinib, also prolonged the survival period of mutant SOD1 Tg mice [24].

Finally, we investigated the postmortem spinal cord tissue of ALS patients. Immunoreactivity of phosphorylated Src was increased in the remaining MNs of ALS spinal cords (fig. S6A, table S6) as well as that of phosphorylated c-Abl [24], although the trend toward increased phosphorylation of Src in whole ALS spinal cords was not significant (fig. S6B). Since phosphorylation of Src was increased in ALS patient iPSC-derived MNs, these results suggest that phosphorylation of Src may occur at early stage in ALS, and that patient iPSCs would be useful to analyze ALS patient MNs at early stage before clinical onset.

confidential

Discussion

We developed a phenotypic screen assay with a readout of MN survival using familial ALS patient iPSCs with mutation in *SOD1*. Using this assay, we showed that Src/c-Abl

inhibitors and the knock-down approach of Src/c-Abl rescued ALS MNs. Further analysis revealed that these drugs promoted autophagy, reduced misfolded SOD1 protein levels, and restored the energy shortage in ALS MNs. Furthermore, treatment with the Src/c-Abl inhibitors rescued other genetic types of ALS MNs including mutant TDP-43-, C9orf72 expansion mediated-familial ALS, and sporadic ALS MNs. Finally, we found that the Src/c-Abl inhibitor prolonged the survival period in ALS model mice.

Mutations in *SOD1* cause its protein-conformational changes, misfolding, and aggregation that are specifically localized in pathologically affected lesions in animal models and human ALS patients [30]. We showed that Src/c-Abl inhibitors reduced misfolded SOD1 level in ALS MNs. As a mechanism for the reduction of misfolded SOD1, we explored proteolysis, observing that Src/c-Abl inhibitors promoted autophagy, which was supported by previous reports of enhancement of autophagy by Src/c-Abl inhibitors [31, 32]. It was demonstrated that misfolded SOD1 induces ER stress, mitochondrial dysfunction [7], and changes in membrane property [33]. We observed ATP shortage in ALS MNs, speculating that misfolded mutant protein provoked ER stress and/or altered the membrane property of hyperexcitability as previously demonstrated [34, 35], and/or caused mitochondrial dysfunction and finally decreased ATP levels (Fig. 3J). Increased gene categories and their reversion by Src/c-Abl inhibition of the TCA cycle and respiratory electron transport explored by our single ALS MN analysis indicated a compensated response against ATP shortage of ALS MNs. A computational model of MN degeneration showed ATP shortage with mitochondrial involvement [36]. We supposed that Src/c-Abl inhibitors restored ATP by autophagy with decreasing misfolded proteins. Furthermore, ATP binding to Src/c-Abl is

confidential

required for its own activation, and Src/c-Abl inhibitors blocked ATP binding [37] and may have contributed to the increases in ATP levels. Although it remains unclear why phosphorylated Src/c-Abl is increased in ALS MNs, as shown both in this study and in a previous report of postmortem ALS patients MNs [24], we speculated that a RTK-mediated mechanism might be associated with Src/c-Abl activation in ALS MNs. The signal activation mechanism, promoted by oligomerized proteins in ALS MNs, may share a mechanism with cancer signaling such as BCR-Abl or EML4-ALK [38]. BCR or EML4 in oncoproteins is dimerized, leading to activation of Abl or ALK and to induction of cell proliferation in dividing cells. In contrast, misfolded proteins associated with RTK may be oligomerized, leading to activation of Src/c-Abl and to induction of neurodegeneration in non-dividing cells, ALS MNs. c-Abl activation is known to result in neurodegeneration of adult mouse neurons [20] and apoptotic response [39].

ALS is a heterogeneous disease, as its various disease phenotypes it has in common are derived from multiple causes including different gene mutations. It is a certainty that multiple molecular mechanisms are involved in the cause of ALS, but these mechanisms remain unknown [2]. Although this heterogeneity of ALS may complicate the identification of prospective therapeutics, the analysis of patient iPSCs from multiple types of ALS should be useful for solving this issue. Our data showed that Src/c-Abl inhibition was effective not only in mutant SOD1 but also in mutant TDP-43 and C9orf72-repeat expansion-associated familial ALS and a part of sporadic ALS MNs. It was reported that TDP-43 formed oligomers that exhibited reduced DNA binding capability and neurotoxicity [40]. C9orf72-repeat expansion formed toxic RNA foci and accumulations of dipeptide repeat protein, which is

confidential

produced via repeat-associated non-ATG translation and causes cytotoxicity [10]. Sporadic ALS is characterized by accumulations of inclusions consisting of TDP-43 in MNs [41], which was also observed in postmortem tissues of the sporadic ALS patient in this study. We observed that these abnormal, misfolded proteins, which contribute to ALS pathogenesis, were decreased by Src/c-Abl inhibitor, and speculated that a common pathway for neuronal death such as the apoptotic pathway would be suppressed by Src/c-Abl inhibitors. Both studies of mutant SOD1 Tg mice with dasatinib and TDP-43 Tg mice with nilotinib/bosutinib showed attenuation of ALS phenotypes, supporting our data [24, 29].

In our screening, the Z' factor was below 0.5, suggesting the assay might not meet a requirement for prevailing standards of compound screening. This score may stem from the fact that the screening takes 7 days to observe cell death without any additional toxins, and this longer than usual period might cause variance of deviations in the assay. Although we confirmed the effect of both Src and c-Abl in siRNA experiments, many kinase inhibitors are not truly selective for a single kinase [42]. The possibility that the efficacy of the drugs on MNs was associated with common off-target effects can also not be ruled out, although we evaluated the protective effects of multiple drugs on MNs, which all had different structures from each other. Furthermore, we also considered that Src and c-Abl may have interacted with each other in the pathway of MN death. Further study would be needed to identify more specific targets between the Src family, including c-Src, Lck, and Lyn [43], and c-Abl.

Since the results of our iPSC study targeted MN survival, we administered one of the hit drugs to ALS model mice from the time point of the beginning of MN death, before clinical onset, to the time point of glial cell involvement. The proper dose of bosutinib for

confidential

mouse experiments could be determined based on the dose of clinical use in humans. Furthermore, the bosutinib dose in this study was used in a previous study [29]. We found that bosutinib delayed the onset of disease and elongated the survival period of mutant SOD1 Tg mice significantly, although the actual improvement of survival of mutant SOD1 Tg mice was modest. These in vivo results confirmed the in vitro data, but also suggested that this drug treatment was not ready for clinical translation. It may be important to examine other doses of bosutinib or other Src/c-Abl inhibitors, such as those showing efficient permeability of the blood-brain barrier, in future studies. Although ALS model mice are useful for evaluating new therapeutics, studies of them might not always predict human responses in clinical trials [44]. It may be important to combine the results of ALS patient iPSCs and ALS model mice simultaneously.

This study indicated that a chemical biology approach with iPSC-based phenotypic screening of existing drugs identified both a converged molecular target and candidate drugs for ALS. We are hopeful that iPSC-based drug repositioning will hasten therapeutic development for ALS.

Materials and Methods

Study design

The objective of our study was to identify a candidate drug or a target for ALS treatment. Through-put drug screening was performed using cellular phenotype of ALS MNs generated from patient iPSCs following disease modeling of ALS. Among hit drugs, candidate targets for ALS treatment were focused upon and validated using multiple ALS iPSC clones. This

confidential

study was extended to ALS model mice to analyze the effects in vivo. Generation and use of human iPSCs was approved by the Ethics Committees of the respective departments including Kyoto University. All methods were performed in accordance with approved guidelines. Formal informed consent was obtained from all subjects. All mice analyzed in this study were cared for, the procedures were performed in accordance with the Kyoto University Animal Institutional Guidelines, and all experiments were approved by the CiRA Animal Experiment Committee. Human postmortem samples with written informed consent were obtained from the Department of Medicine and Graduate Schools of Medicine, Kyoto University, Jichi Medical University, and Kansai Medical University.

Generation of iPSCs

iPSCs were generated from skin fibroblasts, peripheral blood mononuclear cells (PBMCs) or immortalized B-lymphocytes using retrovirus (Sox2, Klf4, Oct3/4, and c-Myc), sendaivirus (Sox2, Klf4, Oct3/4, and c-Myc) or episomal vectors (Sox2, Klf4, Oct3/4, L-Myc, Lin28, and p53-shRNA) as reported previously [45-47], and were cultured on an SNL feeder layer with human iPSC medium (primate embryonic stem cell medium; ReproCELL, Yokohama, Japan) supplemented with 4 ng/ml basic FGF (Wako Chemicals, Osaka, Japan) and penicillin/streptomycin.

Supplementary materials

#. Supplemental materials and methods

#. fig. S1- S6

confidential

#. table S1- S8

Acknowledgements

We would like to express our sincere gratitude to all our coworkers and collaborators including Takako Enami, Ran Shibukawa, Misato Funayama, Mitsuyo Kawada, Kazuya Goto, Henry Houlden, and Elisavet Preza for their technical support. We acknowledge Peter Karagiannis for providing critical reading. The authors are grateful to Noriko Endo, Rumi Ueno, and Rie Okuyama for their administrative support. This work was funded in part by a grant from the iPS Cell Research Fund (S.Y.); Center for iPSC production, The Program for Intractable Diseases Research utilizing Disease-specific iPS cells, Research Center Network for Realization of Regenerative Medicine from the Japan Agency for Medical Research and Development (AMED) (S.Y.); the grant for Core Center for iPS cell Research of Research Center Network for Realization of Regenerative Medicine from AMED (S.Y., H.I.); the Program for Intractable Diseases Research utilizing disease-specific iPS cells from AMED (H.I.); Research Project for Practical Applications of Regenerative Medicine from AMED (H.I); the Mochida Memorial Foundation for Medical and Pharmaceutical Research (H.I.); the Daiichi Sankyo Foundation of Life Science (H.I.). S.Y. is a scientific advisor of iPS Academia Japan without salary.

Contributions

H.I. conceived the project; K.I. and H.I. designed the experiments; K.I., A.W., K.T., T.K., S.K., A.T., T.E., N.O., M.H., H.A., T.A., and H.Ito performed the experiments; K.I., A.W.,

confidential

T.Y., D.W., and H.I. analyzed the data; K.W., A.H., A.O., T. Kunath., S.W., T.E., T.F., H.N., K.H., H.Ichijo, J-P.J., and S.Kaneko contributed reagents, materials and analysis tools; Y.I., M.M., H.T., A.Tamaoka, H.F., K.M., K.O., and R.K. recruited patients; D.W., R.T., and S.Y. provided critical reading and scientific discussions; K.I. and H.I. wrote the paper.

References and Notes:

1. Ling, S.C., Polymenidou, M., and Cleveland, D.W. Converging mechanisms in ALS and FTD: disrupted RNA and protein homeostasis. *Neuron* 79, 416-438 (2013).

2. Ravits, J., Appel, S., Baloh, R.H., Barohn, R., Brooks, B.R., Elman, L., Floeter, M.K., Henderson, C., Lomen-Hoerth, C., Macklis, J.D., McCluskey, L., Mitsumoto, H., Przedborski, S., Rothstein, J., Trojanowski, J.Q., van den Berg, L.H., and Ringel, S. Deciphering amyotrophic lateral sclerosis: what phenotype, neuropathology and genetics are telling us about pathogenesis. *Amyotroph Lateral Scler Frontotemporal Degener* 14 Suppl 1, 5-18 (2013).

3. Rosen, D.R., Siddique, T., Patterson, D., Figlewicz, D.A., Sapp, P., Hentati, A., Donaldson, D., Goto, J., O'Regan, J.P., Deng, H.X., and et al. Mutations in Cu/Zn superoxide dismutase gene are associated with familial amyotrophic lateral sclerosis. *Nature* 362, 59-62 (1993).

4. Gurney, M.E., Pu, H., Chiu, A.Y., Dal Canto, M.C., Polchow, C.Y., Alexander, D.D., Caliendo, J., Hentati, A., Kwon, Y.W., Deng, H.X., and et al. Motor neuron degeneration in mice that express a human Cu,Zn superoxide dismutase mutation. *Science* 264, 1772-1775 (1994).

confidential

5. Egawa, N., Kitaoka, S., Tsukita, K., Naitoh, M., Takahashi, K., Yamamoto, T., Adachi, F., Kondo, T., Okita, K., Asaka, I., Aoi, T., Watanabe, A., Yamada, Y., Morizane, A., Takahashi, J., Ayaki, T., Ito, H., Yoshikawa, K., Yamawaki, S., Suzuki, S., Watanabe, D., Hioki, H., Kaneko, T., Makioka, K., Okamoto, K., Takuma, H., Tamaoka, A., Hasegawa, K., Nonaka, T., Hasegawa, M., Kawata, A., Yoshida, M., Nakahata, T., Takahashi, R., Marchetto, M.C., Gage, F.H., Yamanaka, S., and Inoue, H. Drug screening for ALS using patient-specific induced pluripotent stem cells. *Sci Transl Med* 4, 145ra104 (2012).

6. Bilican, B., Serio, A., Barmada, S.J., Nishimura, A.L., Sullivan, G.J., Carrasco, M., Phatnani, H.P., Puddifoot, C.A., Story, D., Fletcher, J., Park, I.H., Friedman, B.A., Daley, G.Q., Wyllie, D.J., Hardingham, G.E., Wilmut, I., Finkbeiner, S., Maniatis, T., Shaw, C.E., and Chandran, S. Mutant induced pluripotent stem cell lines recapitulate aspects of TDP-43 proteinopathies and reveal cell-specific vulnerability. *Proc Natl Acad Sci U S A* 109, 5803-5808 (2012).

7. Kiskinis, E., Sandoe, J., Williams, L.A., Boulting, G.L., Moccia, R., Wainger, B.J., Han, S., Peng, T., Thams, S., Mikkilineni, S., Mellin, C., Merkle, F.T., Davis-Dusenbery, B.N., Ziller, M., Oakley, D., Ichida, J., Di Costanzo, S., Atwater, N., Maeder, M.L., Goodwin, M.J., Nemesh, J., Handsaker, R.E., Paull, D., Noggle, S., McCarroll, S.A., Joung, J.K., Woolf, C.J., Brown, R.H., and Eggan, K. Pathways disrupted in human ALS motor neurons identified through genetic correction of mutant SOD1. *Cell Stem Cell* 14, 781-795 (2014).

8. Burkhardt, M.F., Martinez, F.J., Wright, S., Ramos, C., Volfson, D., Mason, M., Garnes, J., Dang, V., Lievers, J., Shoukat-Mumtaz, U., Martinez, R., Gai, H., Blake, R., Vaisberg, E., Grskovic, M., Johnson, C., Irion, S., Bright, J., Cooper, B., Nguyen, L.,

confidential

Griswold-Prenner, I., and Javaherian, A. A cellular model for sporadic ALS using patient-derived induced pluripotent stem cells. *Mol Cell Neurosci* 56, 355-364 (2013).

9. Chen, H., Qian, K., Du, Z., Cao, J., Petersen, A., Liu, H., Blackbourn, L.W.t., Huang, C.L., Errigo, A., Yin, Y., Lu, J., Ayala, M., and Zhang, S.C. Modeling ALS with iPSCs reveals that mutant SOD1 misregulates neurofilament balance in motor neurons. *Cell Stem Cell* 14, 796-809 (2014).

10. Donnelly, C.J., Zhang, P.W., Pham, J.T., Haeusler, A.R., Mistry, N.A., Vidensky, S., Daley, E.L., Poth, E.M., Hoover, B., Fines, D.M., Maragakis, N., Tienari, P.J., Petrucelli, L., Traynor, B.J., Wang, J., Rigo, F., Bennett, C.F., Blackshaw, S., Sattler, R., and Rothstein, J.D. RNA toxicity from the ALS/FTD C9ORF72 expansion is mitigated by antisense intervention. *Neuron* 80, 415-428 (2013).

11. Mitne-Neto, M., Machado-Costa, M., Marchetto, M.C., Bengtson, M.H., Joazeiro, C.A., Tsuda, H., Bellen, H.J., Silva, H.C., Oliveira, A.S., Lazar, M., Muotri, A.R., and Zatz, M. Downregulation of VAPB expression in motor neurons derived from induced pluripotent stem cells of ALS8 patients. *Hum Mol Genet* 3642-3652 (2011).

12. Woltjen, K., Michael, I.P., Mohseni, P., Desai, R., Mileikovsky, M., Hamalainen, R., Cowling, R., Wang, W., Liu, P., Gertsenstein, M., Kaji, K., Sung, H.K., and Nagy, A. piggyBac transposition reprograms fibroblasts to induced pluripotent stem cells. *Nature* 458, 766-770 (2009).

13. Ashburn, T.T., and Thor, K.B. Drug repositioning: identifying and developing new uses for existing drugs. *Nat Rev Drug Discov* 3, 673-683 (2004).

14. Brugge, J.S., and Erikson, R.L. Identification of a transformation-specific antigen

confidential

induced by an avian sarcoma virus. *Nature* 269, 346-348 (1977).

15. Greuber, E.K., Smith-Pearson, P., Wang, J., and Pendergast, A.M. Role of ABL family kinases in cancer: from leukaemia to solid tumours. *Nat Rev Cancer* 13, 559-571 (2013).

16. Welch, P.J., and Wang, J.Y. A C-terminal protein-binding domain in the retinoblastoma protein regulates nuclear c-Abl tyrosine kinase in the cell cycle. *Cell* 75, 779-790 (1993).

17. Huang, Y., Yuan, Z.M., Ishiko, T., Nakada, S., Utsugisawa, T., Kato, T., Kharbanda, S., and Kufe, D.W. Pro-apoptotic effect of the c-Abl tyrosine kinase in the cellular response to 1-beta-D-arabinofuranosylcytosine. *Oncogene* 15, 1947-1952 (1997).

18. Mojsilovic-Petrovic, J., Jeong, G.B., Crocker, A., Arneja, A., David, S., Russell, D.S., and Kalb, R.G. Protecting motor neurons from toxic insult by antagonism of adenosine A2a and Trk receptors. *J Neurosci* 26, 9250-9263 (2006).

19. Ellis, C.E., Schwartzberg, P.L., Grider, T.L., Fink, D.W., and Nussbaum, R.L. alpha-synuclein is phosphorylated by members of the Src family of protein-tyrosine kinases. *J Biol Chem* 27, 3879-3884 (2001).

20. Schlatterer, S.D., Acker, C.M., and Davies, P. c-Abl in neurodegenerative disease. *J Mol Neurosci* 45, 445-452 (2011).

21. Dawson, T.M., and Dawson, V.L. Parkin plays a role in sporadic Parkinson's disease. *Neurodegener Dis* 13, 69-71 (2014).

22. Jing, Z., Caltagarone, J., and Bowser, R. Altered subcellular distribution of c-Abl in Alzheimer's disease. *J Alzheimers Dis* 17, 409-422 (2009).

confidential

23. Tremblay, M.A., Acker, C.M., and Davies, P. Tau phosphorylated at tyrosine 394 is found in Alzheimer's disease tangles and can be a product of the Abl-related kinase, Arg. *J Alzheimers Dis* 19, 721-733 (2010).

24. Katsumata, R., Ishigaki, S., Katsuno, M., Kawai, K., Sone, J., Huang, Z., Adachi, H., Tanaka, F., Urano, F., and Sobue, G. c-Abl inhibition delays motor neuron degeneration in the G93A mouse, an animal model of amyotrophic lateral sclerosis. *PLoS One* 7, e46185 (2012).

25. Hester, M.E., Murtha, M.J., Song, S., Rao, M., Miranda, C.J., Meyer, K., Tian, J., Boulting, G., Schaffer, D.V., Zhu, M.X., Pfaff, S.L., Gage, F.H., and Kaspar, B.K. Rapid and efficient generation of functional motor neurons from human pluripotent stem cells using gene delivered transcription factor codes. *Mol Ther* 19, 1905-1912 (2011).

26. Fujisawa, T., Homma, K., Yamaguchi, N., Kadowaki, H., Tsuburaya, N., Naguro, I., Matsuzawa, A., Takeda, K., Takahashi, Y., Goto, J., Tsuji, S., Nishitoh, H., and Ichijo, H. A novel monoclonal antibody reveals a conformational alteration shared by amyotrophic lateral sclerosis-linked SOD1 mutants. *Ann Neurol* 72, 739-749 (2012).

27. Gros-Louis, F., Soucy, G., Lariviere, R., and Julien, J.P. Intracerebroventricular infusion of monoclonal antibody or its derived Fab fragment against misfolded forms of SOD1 mutant delays mortality in a mouse model of ALS. *J Neurochem* 113, 1188-1199 (2010).

28. Yang, Y.M., Gupta, S.K., Kim, K.J., Powers, B.E., Cerqueira, A., Wainger, B.J., Ngo, H.D., Rosowski, K.A., Schein, P.A., Ackeifi, C.A., Arvanites, A.C., Davidow, L.S., Woolf, C.J., and Rubin, L.L. A small molecule screen in stem-cell-derived motor neurons

confidential

identifies a kinase inhibitor as a candidate therapeutic for ALS. *Cell Stem Cell* 12, 713-726 (2013).

29. Wenqiang, C., Lonskaya, I., Hebron, M.L., Ibrahim, Z., Olszewski, R.T., Neale, J.H., and Moussa, C.E. Parkin-mediated reduction of nuclear and soluble TDP-43 reverses behavioral decline in symptomatic mice. *Hum Mol Genet* 23, 4960-4969 (2014).

30. Brotherton, T.E., Li, Y., Cooper, D., Gearing, M., Julien, J.P., Rothstein, J.D., Boylan, K., and Glass, J.D. Localization of a toxic form of superoxide dismutase 1 protein to pathologically affected tissues in familial ALS. *Proc Natl Acad Sci U S A* 109, 5505-5510 (2012).

31. Mahul-Mellier, A.L., Fauvet, B., Gysbers, A., Dikiy, I., Oueslati, A., Georgeon, S., Lamontanara, A.J., Bisquertt, A., Eliezer, D., Masliah, E., Halliday, G., Hantschel, O., and Lashuel, H.A. c-Abl phosphorylates alpha-synuclein and regulates its degradation: implication for alpha-synuclein clearance and contribution to the pathogenesis of Parkinson's disease. *Hum Mol Genet* 23, 2858-2879 (2014).

32. Ertmer, A., Huber, V., Gilch, S., Yoshimori, T., Erfle, V., Duyster, J., Elsasser, H.P., and Schatzl, H.M. The anticancer drug imatinib induces cellular autophagy. *Leukemia* 21, 936-942 (2007).

33. Choi, J., Song, H.D., Lee, S., Yang, Y.I., Nam, J.H., Kim, S.J., Sung, J.J., Kang, T., and Yi, J. Direct observation of defects and increased ion permeability of a membrane induced by structurally disordered Cu/Zn-superoxide dismutase aggregates. *PLoS One* 6, e28982 (2011).

34. Wainger, B.J., Kiskinis, E., Mellin, C., Wiskow, O., Han, S.S., Sandoe, J., Perez,

confidential

N.P., Williams, L.A., Lee, S., Boulting, G., Berry, J.D., Brown, R.H., Jr., Cudkowicz, M.E., Bean, B.P., Eggan, K., and Woolf, C.J. Intrinsic membrane hyperexcitability of amyotrophic lateral sclerosis patient-derived motor neurons. *Cell Rep* 7, 1-11 (2014).

35. Devlin, A.C., Burr, K., Borooah, S., Foster, J.D., Cleary, E.M., Geti, I., Vallier, L., Shaw, C.E., Chandran, S., and Miles, G.B. Human iPSC-derived motoneurons harbouring TARDBP or C9ORF72 ALS mutations are dysfunctional despite maintaining viability. *Nat Commun* 6, 5999 (2015).

36. Le Masson, G., Przedborski, S., and Abbott, L.F. A computational model of motor neuron degeneration. *Neuron* 83, 975-988 (2014).

37. Musumeci, F., Schenone, S., Brullo, C., and Botta, M. An update on dual Src/Abl inhibitors. *Future Med Chem* 4, 799-822 (2012).

38. Soda, M., Choi, Y.L., Enomoto, M., Takada, S., Yamashita, Y., Ishikawa, S., Fujiwara, S., Watanabe, H., Kurashina, K., Hatanaka, H., Bando, M., Ohno, S., Ishikawa, Y., Aburatani, H., Niki, T., Sohara, Y., Sugiyama, Y., and Mano, H. Identification of the transforming EML4-ALK fusion gene in non-small-cell lung cancer. *Nature* 448, 561-566 (2007).

39. Ito, Y., Pandey, P., Mishra, N., Kumar, S., Narula, N., Kharbanda, S., Saxena, S., and Kufe, D. Targeting of the c-Abl tyrosine kinase to mitochondria in endoplasmic reticulum stress-induced apoptosis. *Mol Cell Biol* 21, 6233-6242 (2001).

40. Fang, Y.S., Tsai, K.J., Chang, Y.J., Kao, P., Woods, R., Kuo, P.H., Wu, C.C., Liao, J.Y., Chou, S.C., Lin, V., Jin, L.W., Yuan, H.S., Cheng, I.H., Tu, P.H., and Chen, Y.R. Full-length TDP-43 forms toxic amyloid oligomers that are present in frontotemporal lobar

confidential

dementia-TDP patients. *Nat Commun* 5, 4824 (2014).

41. Neumann, M., Sampathu, D.M., Kwong, L.K., Truax, A.C., Micsenyi, M.C., Chou, T.T., Bruce, J., Schuck, T., Grossman, M., Clark, C.M., McCluskey, L.F., Miller, B.L., Masliah, E., Mackenzie, I.R., Feldman, H., Feiden, W., Kretzschmar, H.A., Trojanowski, J.Q., and Lee, V.M. Ubiquitinated TDP-43 in frontotemporal lobar degeneration and amyotrophic lateral sclerosis. *Science* 314,130-133 (2006).

42. Martin, K.J., and Arthur, J.S. Selective kinase inhibitors as tools for neuroscience research. *Neuropharmacology* 63, 1227-1237 (2012).

43. Boggon, T.J., and Eck, M.J. Structure and regulation of Src family kinases. *Oncogene* 23, 7918-7927 (2004).

44. Rothstein, J.D. Of mice and men: reconciling preclinical ALS mouse studies and human clinical trials. *Ann Neurol* 53, 423-426 (2003).

45. Takahashi, K., Tanabe, K., Ohnuki, M., Narita, M., Ichisaka, T., Tomoda, K., and Yamanaka, S. Induction of pluripotent stem cells from adult human fibroblasts by defined factors. *Cell* 131, 861-872 (2007).

46. Okita, K., Yamakawa, T., Matsumura, Y., Sato, Y., Amano, N., Watanabe, A., Goshima, N., and Yamanaka, S. An efficient nonviral method to generate integration-free human-induced pluripotent stem cells from cord blood and peripheral blood cells. *Stem Cells* 31, 458-466 (2013).

47. Fusaki, N., Ban, H., Nishiyama, A., Saeki, K., and Hasegawa, M. Efficient induction of transgene-free human pluripotent stem cells using a vector based on Sendai virus, an RNA virus that does not integrate into the host genome. *Proc Jpn Acad Ser B Phys Biol*

confidential

Sci 85, 348-362 (2009).

confidential

Figure Legends

Fig. 1. Generation of MNs using transcription factors and modeling ALS-MNs

A. Protocol for MN generation. Scale bars, 10 μm.

B. Generated MNs present spinal MN markers HB9, ChAT, and SMI-32. Scale bars, 10 μm.

C. Real-time PCR analysis shows increase in mRNA levels of HB9 and ChAT on Day 7 (each group represents mean ± SEM, n = 3; Student *t*-test, *p<0.05).

D. Co-cultures with human myoblasts, Hu5/E18. Neurites of MNs co-localized with α-bungarotoxin-labeled acetylcholine receptors. Scale bar, 10 μm.

E. Action potentials from current clamp recordings.

F. Functional neurotransmitter receptors on generated MNs evaluated by electrophysiological analysis. Addition of 500 μM glutamate, 500 μM kainate, or 500 μM GABA induced inward currents during voltage clamp recordings.

G. The percentage of HB9-positive cells on Day 7 (each group represents mean ± SEM, n = 3).

H. Modeling ALS MNs. Misfolded SOD1 protein accumulated in MNs with mutant SOD1 gene. Scale bars, 10 μm.

I. Accumulations of misfolded SOD1 protein were shown in mutant SOD1 ALS MN culture using immunoprecipitation assay.

J,K. MN survival assay. Numbers of MNs on Day 7 and on Day 14 were counted by high-content analysis, and the ratio of surviving MNs (Day 14/Day 7 (%)) is shown. The surviving ratio was decreased in mutant SOD1 (L144FVX) compared with control and mutation-corrected clone (each group represents mean ± SEM, n = 6; one-way ANOVA, p<0.05,

confidential

*p<0.05). Scale bars, 10 μm.

Fig. 2. Phenotypic screening using ALS MNs and identification of therapeutic targets

A. Overview of screening flow for ALS MN survival assay.

B. Through-put screening using MNs with mutant SOD1 gene (L144FVX). 1,416 compounds consisting of existing drugs and clinical trial-testing drugs were screened. Scatter plots show screening results and the highlighted compounds shown in Fig. 2D.

C. Representative figures of assay results. Treatment with bosutinib increased MN survival. Scale bar, 100 μm.

D. Hit drugs showed dose-dependent effects (each group represents mean ± SEM, n = 6; one-way ANOVA, p<0.05, *p<0.05).

E. Targets of hit drugs. 14 of 27 hit drugs were included in receptor tyrosine kinase (RTK) and Src/c-Abl-associated signaling pathways. PKC; protein kinase C.

F. Knock-down of Src or c-Abl increased the survival rate of mutant SOD1 ALS MNs (ALS1) (each group represents mean ± SEM, n = 6; one-way ANOVA, p<0.05, *p<0.05).

G,H. Phosphorylation of Src/c-Abl was increased in mutant SOD1 ALS MNs, and bosutinib inhibited this phosphorylation according to western blot analysis (each group represents mean ± SEM, n = 3; two-way ANOVA, p<0.05, *p<0.05).

I. Typical figures of immunocytostaining of p-Src/p-c-Abl in MNs. Scale bars, 10 μm.

J. Increase of phosphorylation of Src/c-Abl was inhibited by treatment with bosutinib according to ELISAs (each group represents mean ± SEM, n = 3; two-way ANOVA, p<0.05, *p<0.05). bos; bosutinib.

confidential

Fig. 3. Mechanistic analysis of neuroprotective effects of Src/c-Abl inhibitors on mutant SOD1 ALS MNs

A,B. Bosutinib treatment decreased the amount of p62, which was increased in mutant SOD1 MN culture, and attenuated the ratio of LC3-II/LC3-I (each group represents mean ± SEM, n = 3; two-way ANOVA; $p<0.05$, $*p<0.05$).

C. Increase of p62 was exhibited in mutant SOD1 ALS MNs by ELISAs, and bosutinib treatment decreased the amount of p62 (each group represents mean ± SEM, n = 3; two-way ANOVA; $p<0.05$, $*p<0.05$).

D. Rapamycin increased survival rate of mutant SOD1 ALS MNs (ALS1) (each group represents mean ± SEM, n = 6; one-way ANOVA, $p<0.05$, $*p<0.05$).

E. Knock-down of mTOR increased survival rate of mutant SOD1 ALS MNs (ALS1) (each group represents mean ± SEM, n = 6; Student *t*-test, $p<0.05$).

F. Autophagy inhibitors, LY294002 and chloroquine, decreased the protective effect of bosutinib on MN survival assay (each group represents mean ± SEM, n = 6; two-way ANOVA, $p<0.05$, $*p<0.05$).

G, H. Immunoprecipitation analysis (G) and ELISA (H) showed that bosutinib treatment decreased the misfolded SOD1 protein level, which was elevated in mutant SOD1 MN culture.

I. Bosutinib treatment did not decrease SOD1 mRNA expression level.

J. Intracellular ATP level was decreased in mutant SOD1 MN culture. Bosutinib partially attenuated the ATP shortage (each group represents mean ± SEM, n = 6, Two-way ANOVA;

confidential

p<0.05, *p<0.05).

K. Gene Set Enrichment Analysis of single-cell RNA sequencing showed up-regulation for genes in TCA cycle and respiratory electron transport (control 1; n = 10, control 2; n = 11, ALS1; n = 23, ALS3; n = 21). bos; bosutinib.

Fig. 4. Effect of Src/c-Abl inhibitor on iPSC-derived MNs with different genotypes and on ALS model mice

A. iPSC-derived MNs of each clone on Day 7. Scale bars, 100 μm.

B. Bosutinib increased MN survival of mutant TDP-43-, and C9orf72-repeat expansion-mediated familial ALS and from a part of sporadic ALS (each group represents mean ± SEM, n = 6; one-way ANOVA, p<0.05; post hoc test, p<0.05).

C. Kaplan-Meier analysis showed that bosutinib delayed disease onset of mutant SOD1 Tg mice (bosutinib; 123.2±9.1 days, vehicle; 112.4±14.4 days, mean ± SD, log-rank test, p=0.0021, n = 26 per group).

D. Kaplan-Meier analysis showed that bosutinib extended the survival time of mutant SOD1 Tg mice (bosutinib; 164.1±9.4 days, vehicle; 156.3±8.5 days, mean ± SD, log rank test, p=0.0019, n = 26 per group).

E. Misfolded SOD1 protein in spinal cord at 12 weeks of age was evaluated by ELISA. Bosutinib decreased the misfolded SOD1 accumulations in spinal cord (each group represents mean ± SEM, non-transgenic littermates (non-Tg); n = 3, Tg treated with vehicle; n = 3, Tg treated with bosutinib; n = 3, one-way ANOVA, p<0.05; post hoc test, p<0.05).

F. Typical image of Cresyl violet-stained section of ventral horn from the lumbar spinal cord

confidential

at the late symptomatic stage. Scale bars, 50 μm.

G. The number of MNs on one side of the lumbar spinal cord was quantified (each group represents mean ± SEM, non-Tg; n = 4, Tg treated with vehicle; n = 5, Tg treated with bosutinib; n = 5, one-way ANOVA; $p<0.05$, $*p<0.05$). bos; bosutinib.

confidential

Fig. 1

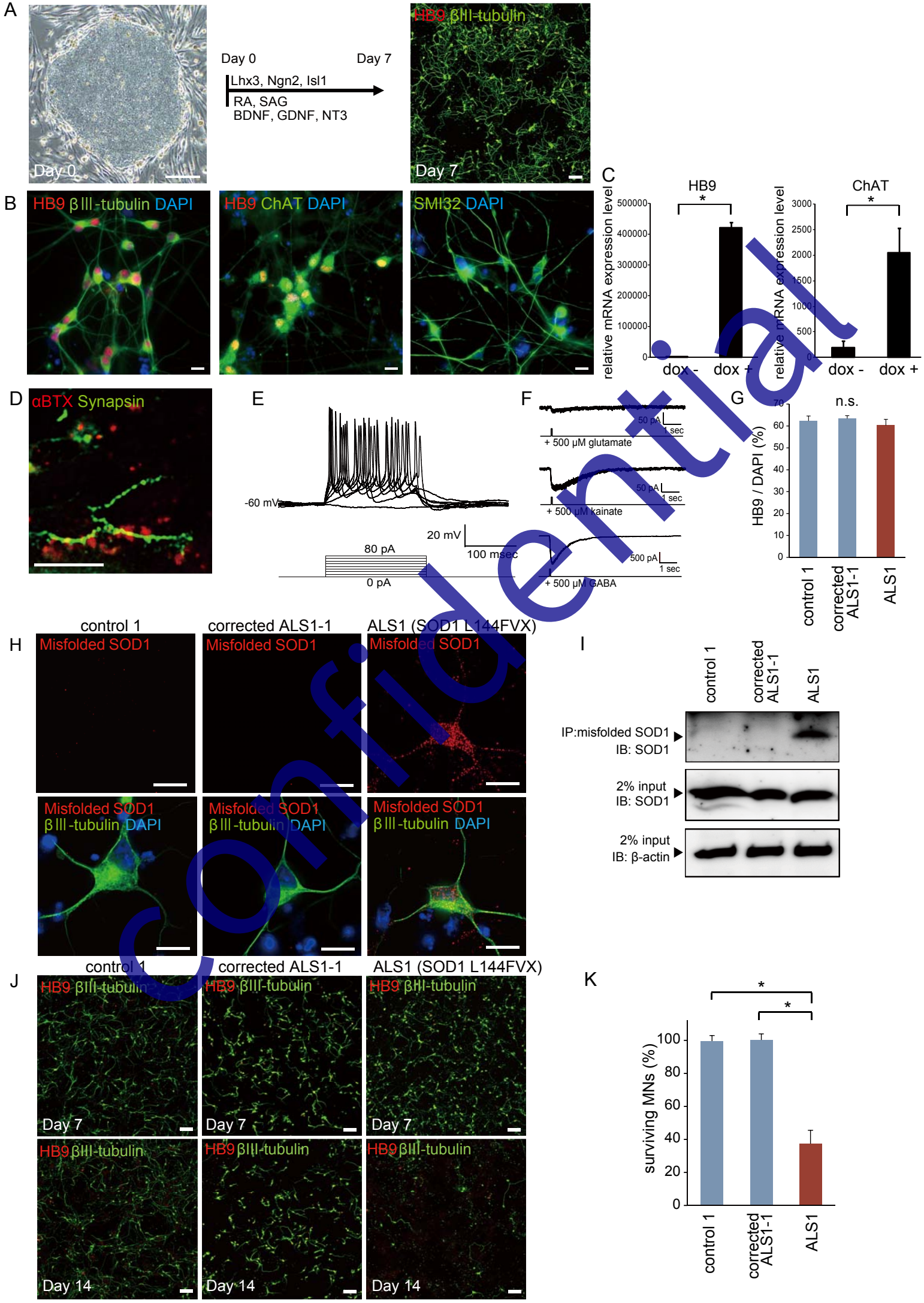

Confidential

Fig. 2

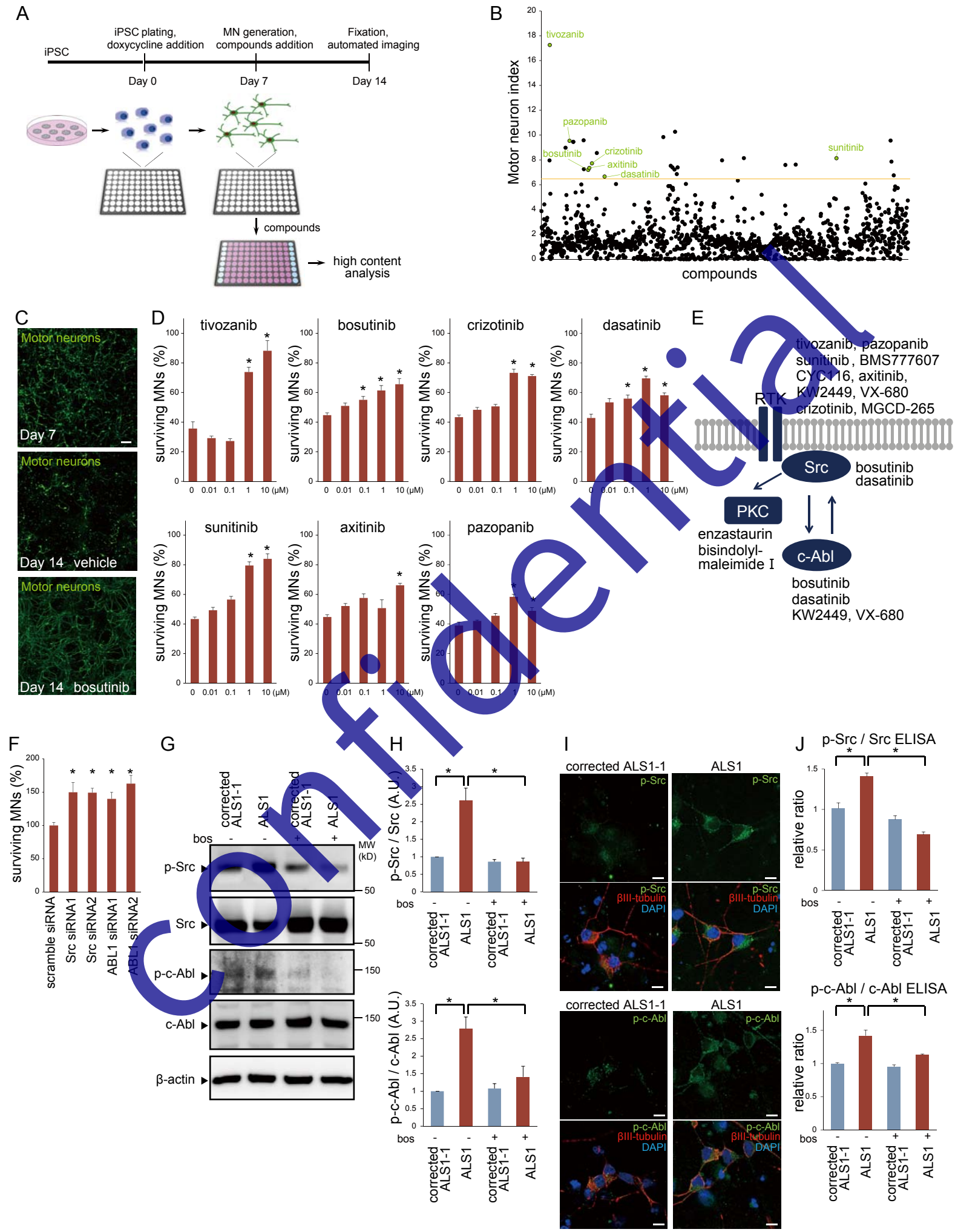

Confidential

Fig. 3

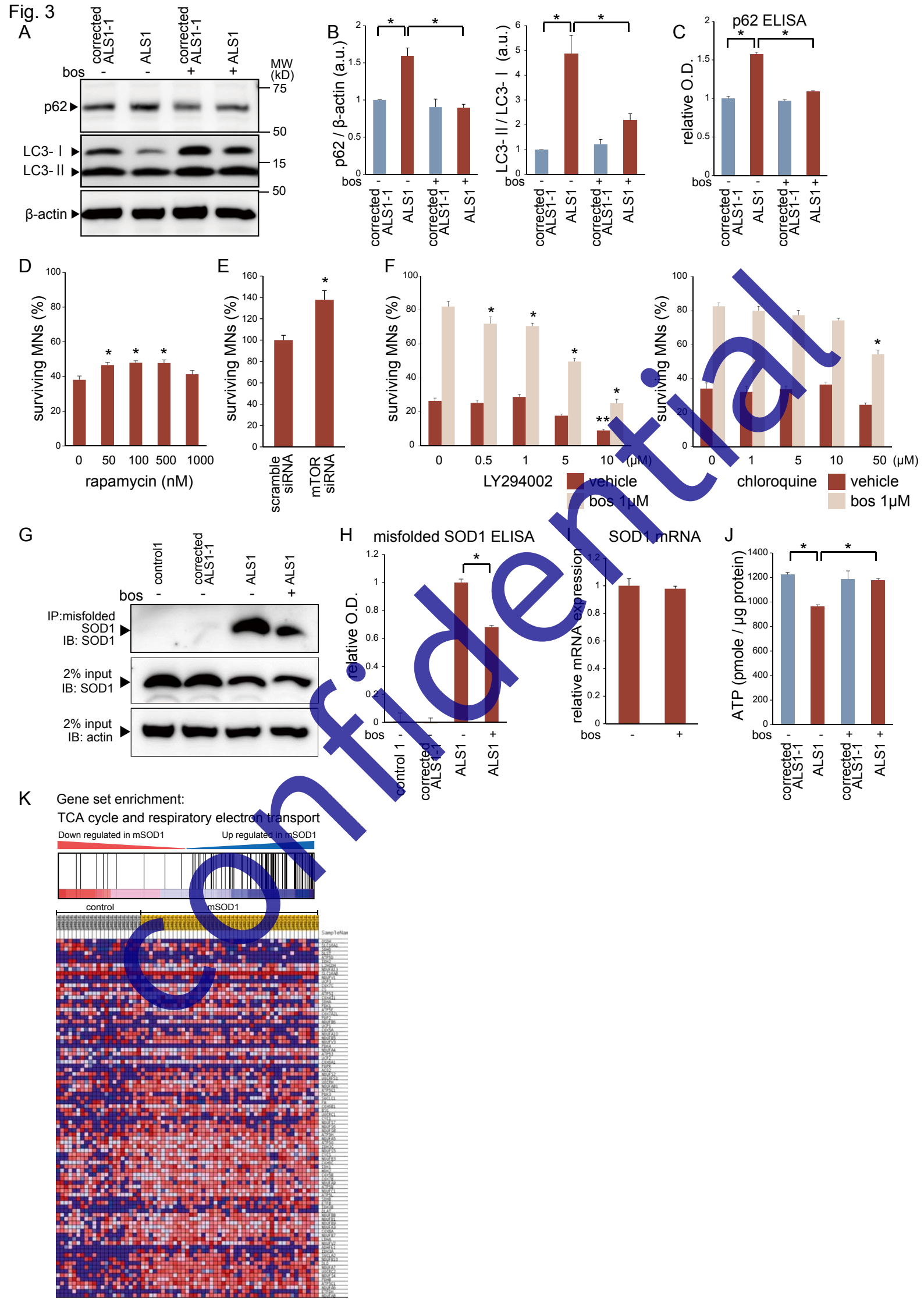

Confidential

Fig. 4

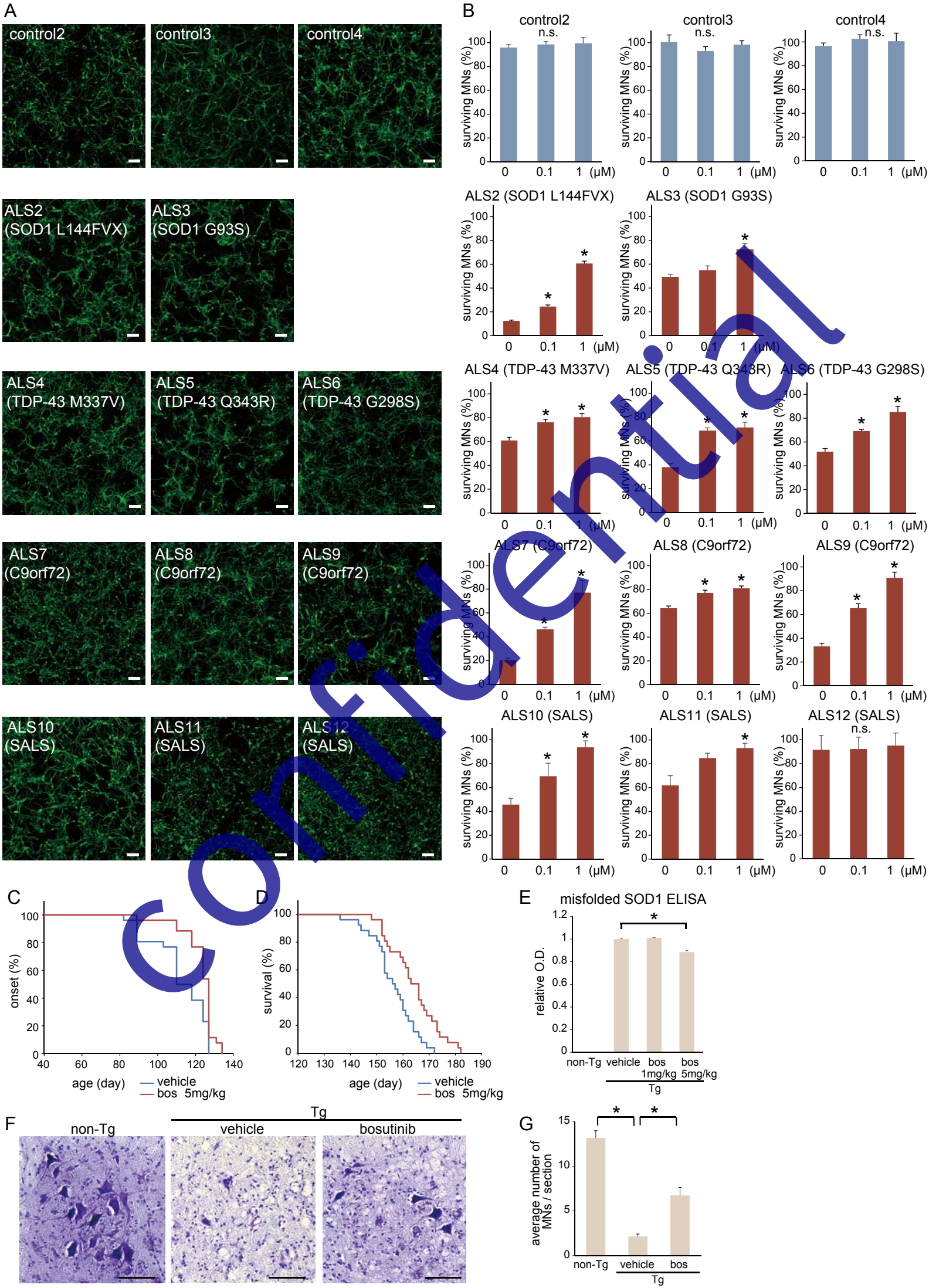

confidential

Fig. S1

A

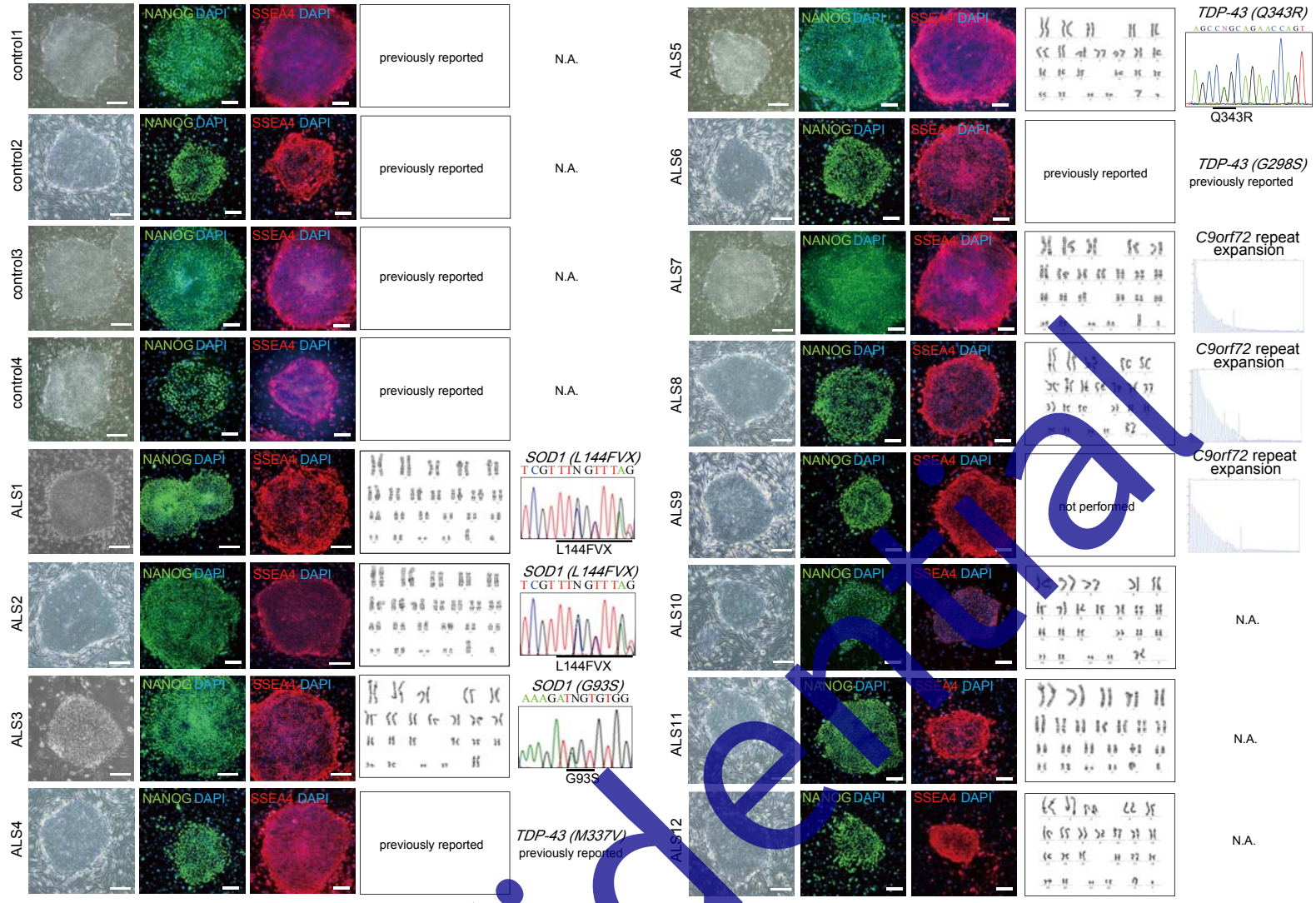

B

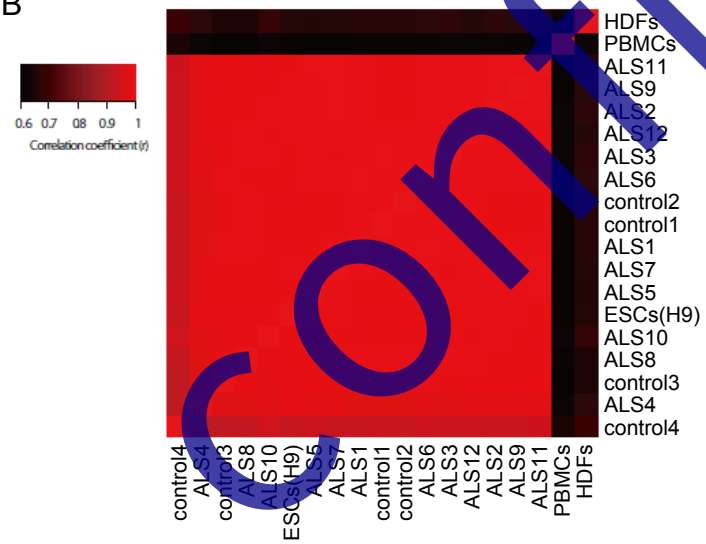

C

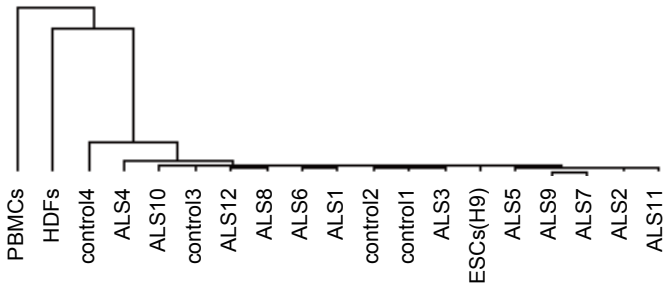

D

	control4	ALS4	control3	ALS8	ALS10	ALS1	control1	control2	ALS6	ALS3	ALS12	ALS2	ALS9	ALS11	ESC(H9)	ALS5	ALS7	PBMCs	HDFs
control4	1																		
ALS4	0.925307	1																	
control3	0.925054	0.97621	1																
ALS8	0.928511	0.97709	0.988603	1															
ALS10	0.948683	0.97888	0.980912	0.984706	1														
ALS1	0.936783	0.977086	0.991236	0.991662	0.989208	1													
control1	0.936915	0.9777	0.990245	0.993358	0.98954	0.993107	1												
control2	0.935476	0.976924	0.990122	0.993055	0.98852	0.99233	0.992473	1											
ALS6	0.94732	0.978577	0.991119	0.989843	0.990734	0.994771	0.992724	0.991661	1										
ALS3	0.942633	0.979394	0.989608	0.991816	0.990771	0.992021	0.994007	0.993438	0.993549	1									
ALS12	0.93993	0.98267	0.989002	0.993174	0.988696	0.99308	0.990998	0.991298	0.992629	0.992214	1								
ALS2	0.939449	0.981924	0.989805	0.990302	0.991532	0.993469	0.990721	0.9903	0.992558	0.992416	0.993764	1							
ALS9	0.939014	0.982494	0.987981	0.989873	0.988971	0.992662	0.989246	0.987724	0.992097	0.991219	0.993079	0.994475	1						
ALS11	0.943129	0.980364	0.989722	0.988689	0.988824	0.991777	0.988316	0.989821	0.993158	0.990778	0.992581	0.994466	0.994784	1					
ESC(H9)	0.933664	0.986654	0.98612	0.988522	0.987589	0.987571	0.987805	0.986184	0.988341	0.989631	0.991439	0.992405	0.992065	0.99048	1				
ALS5	0.942447	0.980427	0.990703	0.989559	0.987272	0.989982	0.990168	0.989996	0.992588	0.992604	0.991105	0.992058	0.993361	0.99391	0.989746	1			
ALS7	0.936718	0.981241	0.987763	0.9896	0.987759	0.99251	0.988245	0.988738	0.992062	0.988742	0.991944	0.993958	0.994861	0.994098	0.990821	0.991849	1		
PBMCs	0.64944	0.621913	0.605631	0.613815	0.625985	0.613614	0.613736	0.614592	0.619966	0.621087	0.624677	0.623309	0.617125	0.620638	0.618981	0.611181	0.608169	1	
HDFs	0.697716	0.673657	0.655371	0.654277	0.689135	0.66712	0.667347	0.666196	0.675544	0.678631	0.664652	0.677217	0.671416	0.669136	0.664283	0.662927	0.665265	0.626551	1

confidential

Fig. S2

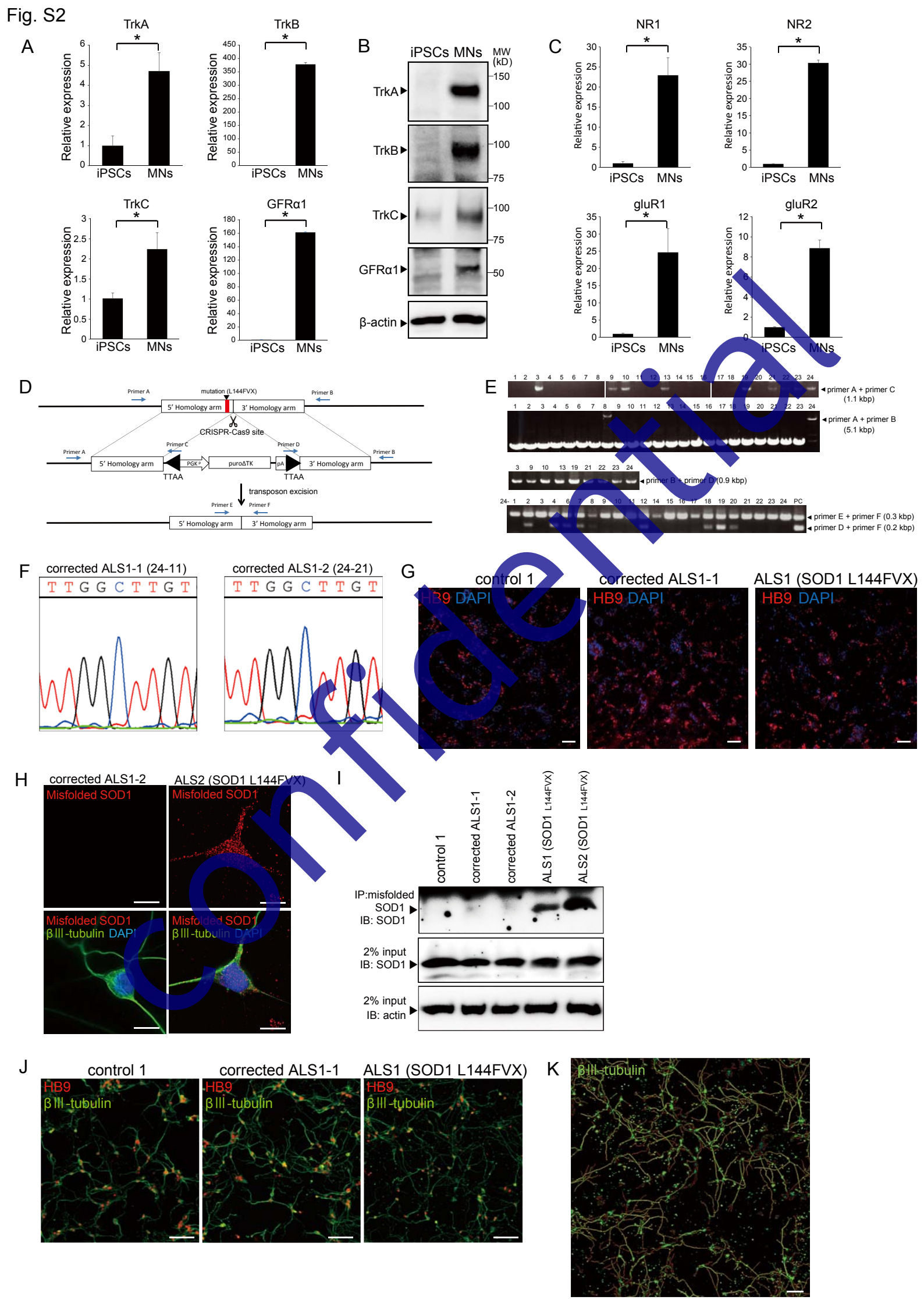

confidential

Fig. S3

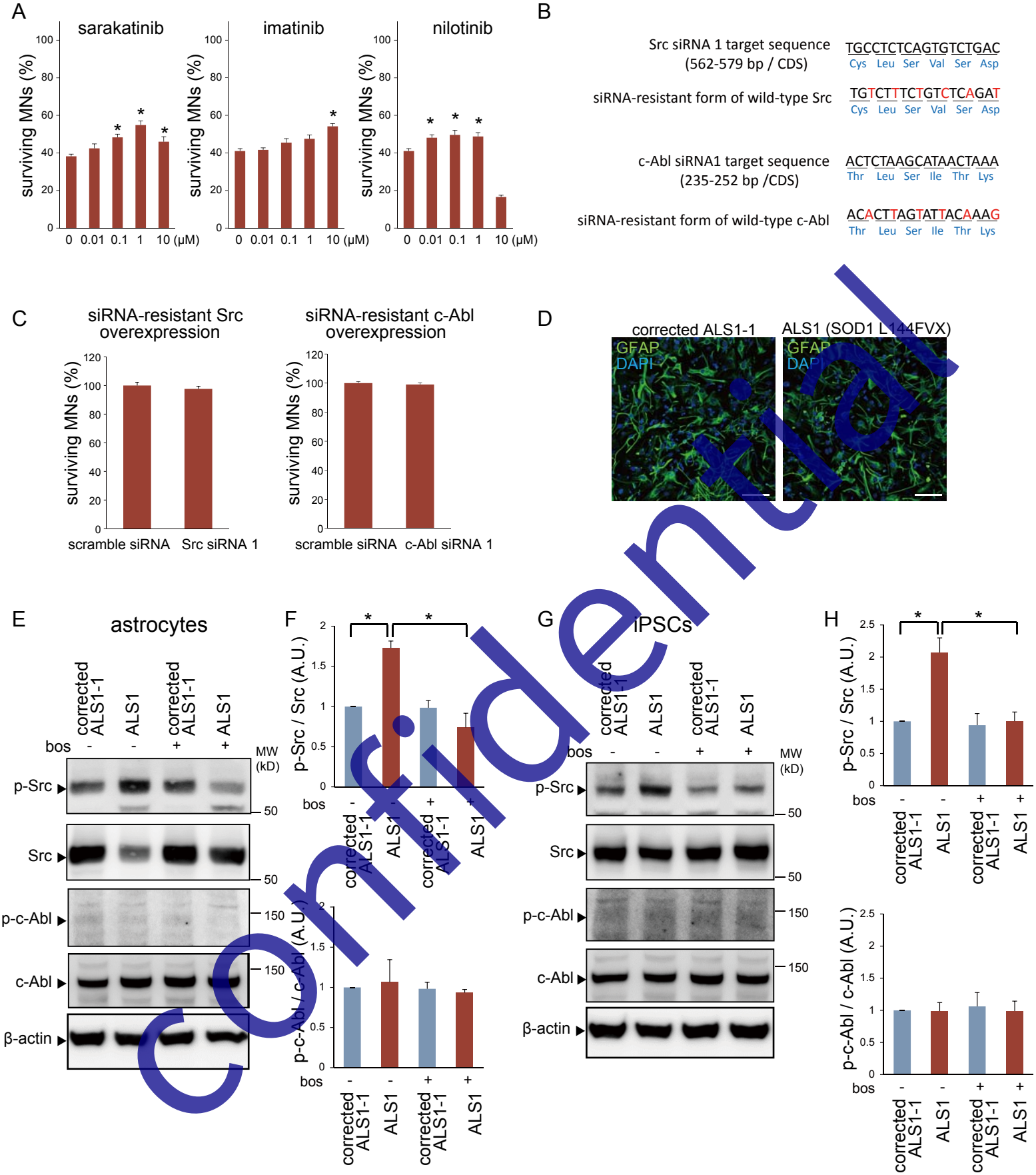

confidential

Fig. S4

Gene set enrichment:
TCA cycle and respiratory electron transport

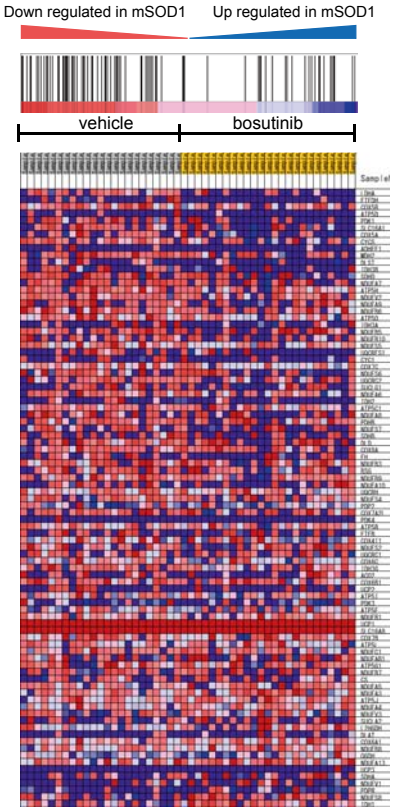

confidential

Fig. S5

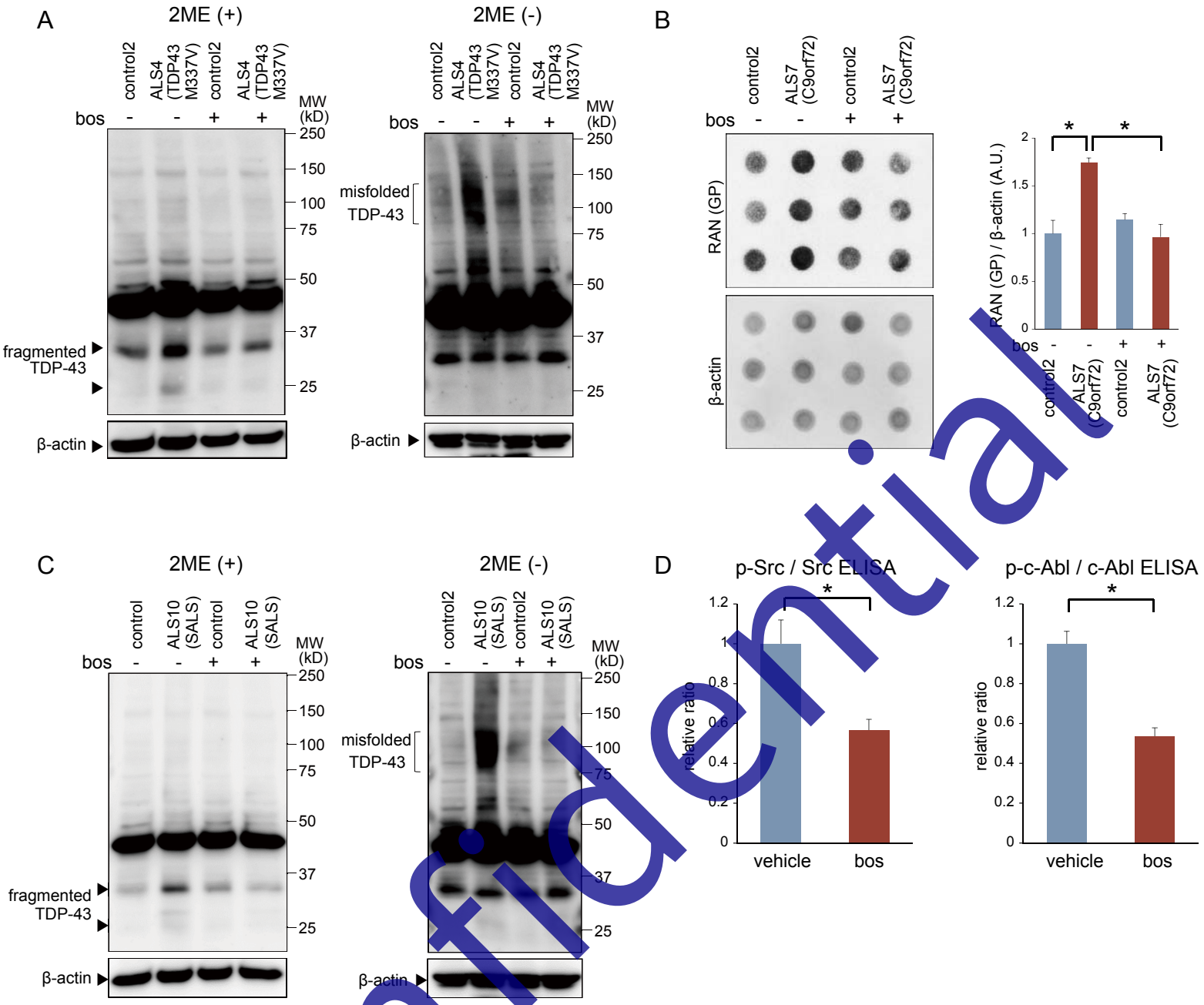

confidential

Fig. S6

A

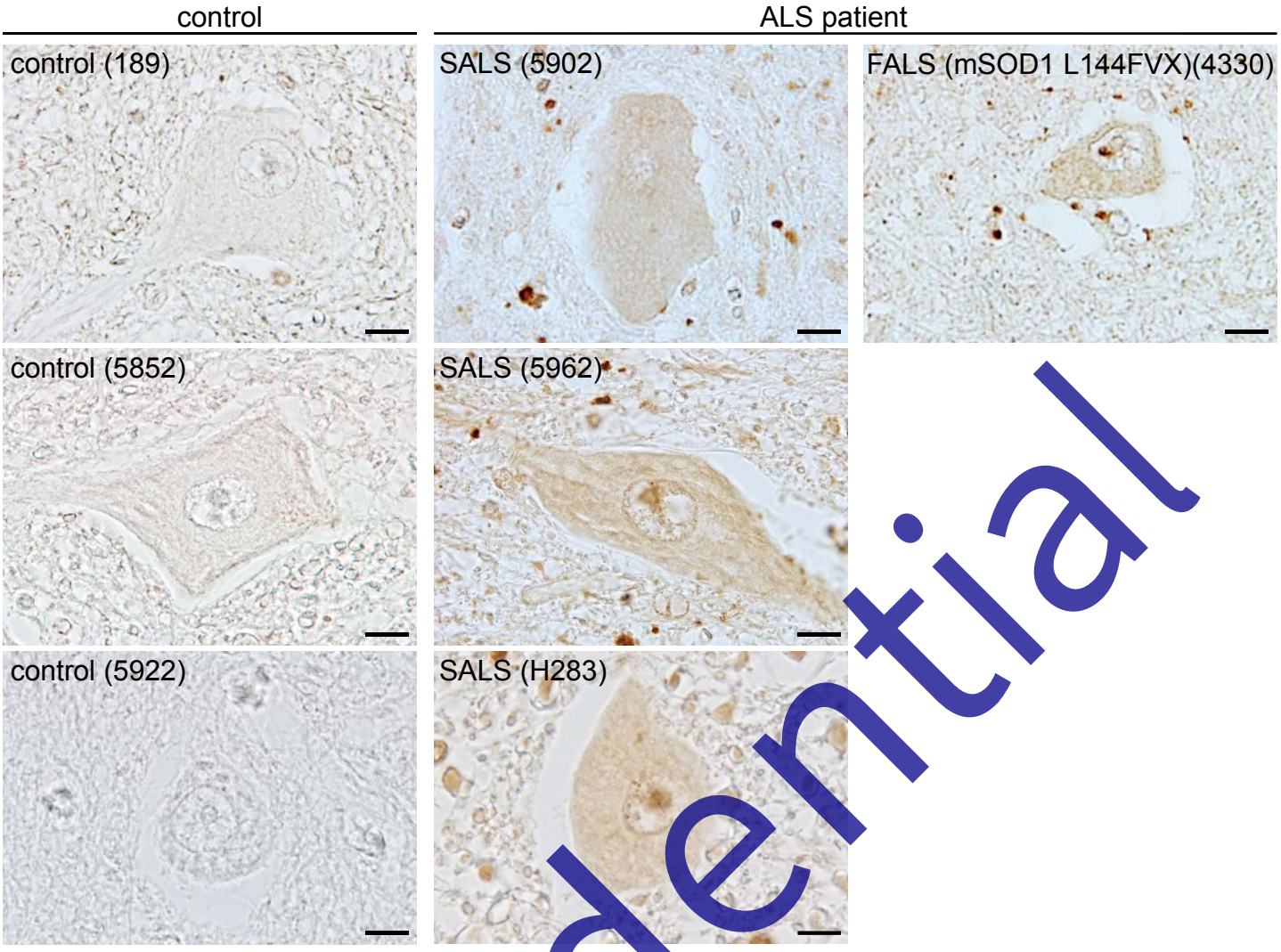

B

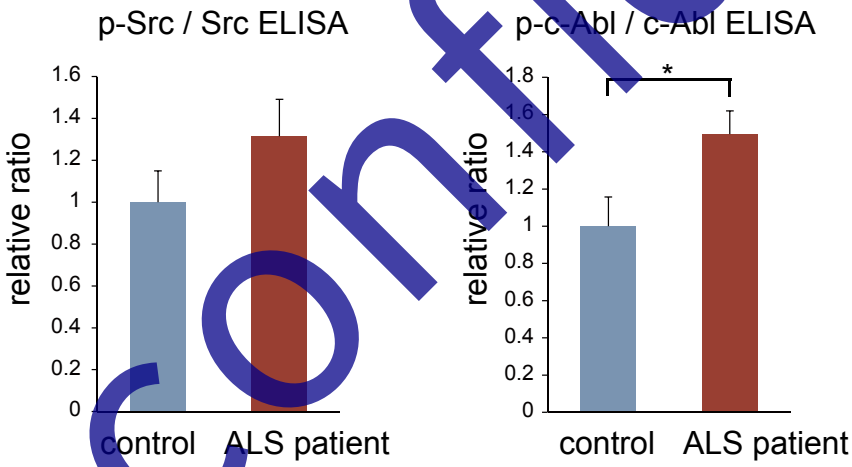

Confidential